A 3D Antenna Array based Solar Cell Integration for Modern MIMO Systems

Ammar Al-Adhami, Yasir Al-Adhami, and Taha A. Elwi

Abstract—**In this work, a design of a 3D array antenna based solar panel integration for self-powered applications in modern wireless communication network. Such array configuration is proposed for Multi Input Multi Output (MIMO) applications. The proposed antenna array is structured as a cubical geometry integrated to a solar panel. Such integration is employed to achieve a self-powered node. The proposed antenna is designed to perform an excellent size reduction at sub-6GHz frequency bands when designed with the aid of the metamaterial (MTM) structures. The antenna performance is enhanced by Moore fractal geometry based on electromagnetic band gap (EBG) defects in the ground plane. The proposed antenna is found to provide a moderate gain at 3.6GHz, 3.9GHz, and 4.9GHz. The antenna array shows low coupling effects, below -20dB, due the array configuration in a cubical shape arrangement. The proposed work is extended to evaluate effectively the bit error rate (BER) and channel capacity (CC), when the proposed antenna system is located in real world communication environments. Therefore, QPSK modulation scheme is considered to suite the applications of 5G systems. The amount of the harvested solar energy is considered the limit to manage the total signal to noise ratio (SNR) in that is applied to the proposed communication scheme. This work is considered for practical aspect issues that is related with amount for the generated power from such integration with solar panel and the total generated SNR. Finally, the comparison between measured and simulated data reveals an excellent agreement between them.**

Index Terms—**SNR, MIMO, self-powered, MTM.**

I. Introduction

Fifth generation (5G) was developed technology of mobile broadband communication that is planned to use after 2020 [1]. The frequency spectrum of 5G systems is used two ranges, sub-6 GHz that is including (3 GHz -to- 6 GHz) and above-6 GHz according to study of physical properties [2]. Different 5G antenna designs were proposed for 5G specifications [3]. The authors attempted to produce the exhaustive review that covered vary important antenna design and its parameters and performances enhancement such as gain, bandwidth and radiation patterns [4]. A monopole antenna array design based on fractal geometry was proposed for MIMO applications [4]. In [5], an antenna structure was consistent of a traditional monopole antenna; this antenna was attached to a fractal patch and mounted on an FR4 substrate to provide broadside radiation patterns as the result of fractal geometry addition with excellent bandwidth.

Manuscript received June 19, 2022; revised July 26, 2023. Date of publication 2023. Date of current version August 1, 2023.

First author is with Al-karkh University of Science, Baghdad, Iraq. (e-mail: ammarisam@kus.edu.iq).

Second author is with the Institute of Technology - Baghdad, Middle Technical University, Baghdad, Iraq. (e-mail: yasir_isam@mtu.edu.iq).

Third author is with the International Applied and Theoretical Research Center (IATRC), Baghdad Quarter, Iraq. (e-mail: taelwi82@gmail.com).

DOI: 10.36244/ICJ.2023.4.2

A multiband fractal at sub-6 GHz microstrip antenna utilizing circle and triangle fractals for different wireless applications to cover three frequency bands of (1.8-2.9GHz, 3.4–4.6 GHz, and 5–5.6 GHz) was proposed in [6]. by loading Koch fractal geometry on edges of a square microstrip patch antenna to enhance the antenna bandwidth and gain by suppressing the surface wave effects [7]. A multiband reconfigurable antenna for sub-6GHz 5G wireless communication networks was designed to control the frequency resonance using pin diodes [8] at two frequency bands.

In another concept, the introduction of the solar panel to the modern antenna designs has become the most urgent for the self-powered wireless systems [9]. For this, MTM based antennas were integrated with solar panels in different publications [10]-[13]. For instance, the authors in [10] proposed an antenna design based on MTM for gain enhancements by integration their antenna design with the solar panel as a substrate. Furthermore, another design was suggested in [11] to integrate the solar panel as a reflector for a Vivaldi antenna based corrugated grating patch with MTM. In [12], a design of MTM structure based on plasmonic antenna array for modern applications; in that design, the authors printed their antenna array on a flexible solar panel. The design of an antenna based MTM in [13] was introduced for self-powered wireless systems by attaching the antenna ground plane to the solar panel.

Later, researchers explored another technique to harvest the green energy from an arterial resource based on RF energy bands [14]. In such technology, the antenna design was introduced with certain specifications such as: High gain-bandwidth products to improve reception efficiency [15], unidirectional radiation patterns to ensure the locus independency [16], and size reduction to ensure system embedding and compatibility with miniaturized electronic circuits [17]. Nonetheless, the matching impedance between the proposed antenna with respect to the rectifier circuit is an important issue to ensure the rectification efficiency of the resulted structure [18].

Recently, several researchers have exploited fractal geometries in microwave circuits, such as antenna designs [19] and microwave filters [2]. To make microwave resonators, fractal geometries may be constructed from a variety of forms [21]. One of the most well-known is the Koch-fractal geometry, which has been adopted as a standard in microwave applications [22]-[29]. In [22-23], a modified Koch-fractal geometry was used to create microstrip band-stop filters. In [24-27], Koch and Minkowski showed how to make MIMO microstrip antenna arrays using fractal geometries. The Koch fractal geometry was utilized to uncouple side lengths of a triangular patch resonator to build a compacted dual-mode band reject filter [28]. A 1D Koch fractal electromagnetic bandgap structure was proposed by [29].

To replace typical ground plane hole etching, a 1D Koch fractal electromagnetic bandgap structure was presented in [30]. The self-similar and space-filling properties of Koch fractal geometry were used to build a monopole antenna [31] based on a tri band for MIMO antenna applications. An octagonal shaped fractal Ultra-Wide Band (UWB) MIMO antenna was designed employing Minkowski fractal geometry of an octagonal form to achieve high downsizing factor with a bandwidth enhancement [32]. Microwave antenna designs might be employed in 5G [33] applications that need high antenna gain [34]. Due to propagation losses, several governments are unwilling to allot microwave bands for 5G potential uses; as a response, high-gain antenna designs have been proposed to avoid this difficulty with little propagation loss [35]. As a result, the sub-six-GHz band has been largely recognized as the preferred frequency range for 5G cellular communication systems [36]. Endfire antenna designs were one of the top competitors to satisfy 5G potential criteria due to their high gain bandwidth offers [37].

The proposed work is organized as following: In section II, the antenna array details are presented with all relative geometrical dimensions. The two scenario of array design two dimensions and three dimensions methodology are discussed in section III, section IV showed the effects of solar cell on antenna performance and channel performance. Finally, the conclusion of this work is presented in section V.

II. Antenna Array Design Details

The proposed antenna array is designed based on a fractal geometry that is proposed for self-powered applications [1]. The antenna array structure is consistent of four printed circuit antennas. The antenna elements are arranged as a cubic array as be shown in Fig. 1. The individual antenna element design is based on four Moore fractal inclusions fed with a coplanar waveguide (CPW) microstrip line. The resulted design is matched to a circuit load with a transmission line as seen in Fig. 1(a). The advantages of the Moore fractal, see Fig. 1(a), introduction are to increase the antenna size reduction and realize multiband resonances as MTM inclusion in the patch [13]. The antenna is printed on an FR4 Techtronic epoxy substrate with dimensions of 22×22×30mm^3. A bandwidth enhancement is achieved within a limited area by magnifying surface current that is afforded on electrically long path [14]. The proposed CPW is used to avoid the capacitive coupling between antenna element and the ground plane [15]. Nevertheless, such design maintains the other surface of the antenna substrate without any printed circuit to be used for busing electronic circuit [16]. The transmission line is designed with width of (0.84mm) to realize 50Ω match circuit and to transfer the surface current motion to the proposed Moore structure [17]. The air gap on the transmission line is introduced to force the current motion toward the fractal geometry as explained in [16]. The antenna ground plane is covered with EBG layer to avoid surface wave retardation that could be created in an opposite interference and inductive loss due to the use of the transmission line junction that can be removed by the capacitive effects of the matching circuit [18]. The proposed EBG is introduced to suppress the surface waves from the antenna edges those effects negatively on the radiation efficiency [19]. The microstrip patch is printed on the FR4 substrate without a ground plane. The substrate dielectric constant is 4.3 with height of 1.67mm. This antenna provides the broadside radiation patterns to cover the tangential components of the antenna radiations [2]. The proposed antenna for this study; three different configurations as 1D, 2D, and 3D as shown in Figs. 1(b), 1(c), and 1(d). The antenna is fabricated on the FR-4 substrate as shown in Fig. 1(e). The antenna ground planes are connected to avoid charges accumulations on the antenna body after introducing the solar panel [20]. The solar panel is mounted on top of the antenna structure as shown in Fig. 1(f).

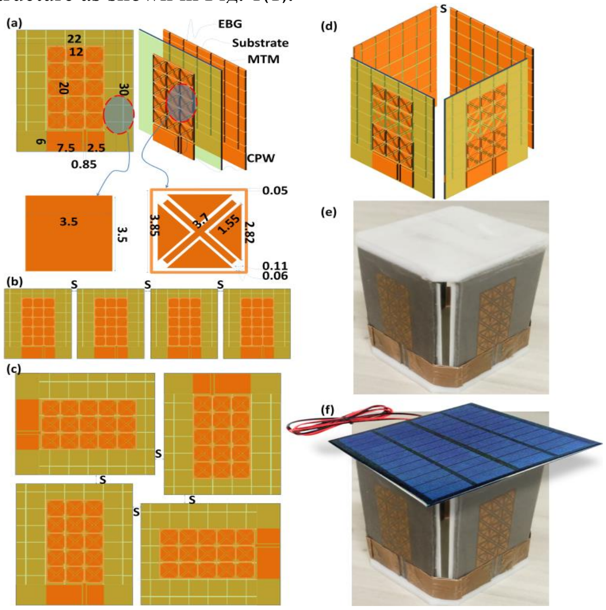

Fig. 1. Antenna array design (a) Front and back side (b) Moore fractal unit cell (c) Cubic antenna array (d) Feed port

III. Array Design Methodology

A- Single Antenna Design

The proposed antenna structure is consistent of four main parts: The first one is patch stricture without MTM circuitries as (case_1). The second case (case_2) is based on the MTM based on Moore geometry introduction with the patch layer. The introduction of the partial ground plane structure to the proposed design is called (case_3).

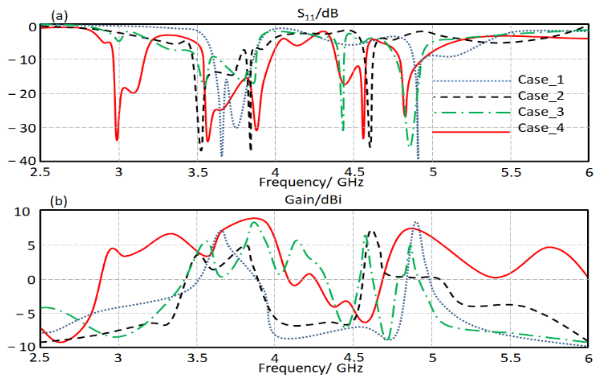

Fig. 2. Antenna performance based on a single antenna element: (a) S_{11} and (b) Gain

The proposed antenna structure based on EBG layer in Fig. 1(a) is presented in (case_4) after the matching circuit introduction. The proposed cases performances are calculated numerically using CST MWS in terms of S_{11} and gain spectra as shown in Fig. 2. Based on the evaluated results, it is found that the proposed antenna bandwidth is enhanced significantly after introducing are matching circuit to design in case_4 with maximum gain of 7.5dBi at 3.83GHz and 4.75GHz. However, the first mode is generated, at 2.96GHz, from the Moore fractal structure introduction. The other two modes were generated from the proposed designs in case_2 and case_3. The fundamental modes are generated by case_1 due to the current motion in the fractal geometry [22].

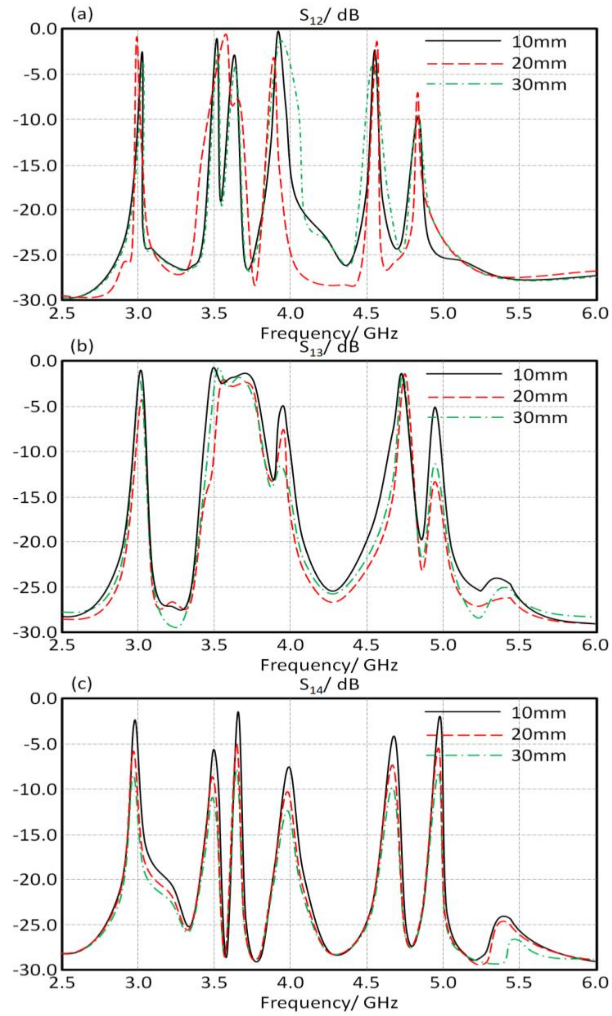

Fig. 3. Coupling effects of 1D configuration in terms of: (a) S_{12}, (b) S_{13}, and (c) S_{14} spectra.

B- Array Design

The proposed antenna is arranged with 1D, 2D, and 3D array scenarios. At beginning, four antenna elements are arranged with different separation distances between the antenna elements as presented in Fig. 1(b). The proposed scenarios at different separation distance are included to realize the effects of that between the mutual coupling spectra only in terms of S_{12} in Fig. 3(a), S_{13} in Fig. 3(b), and S_{14} Fig. 3(c). Therefore, the separation distances (s) are changed from 10 to 30mm with a step 10mm. It is found after reaching 30mm distance, the mutual coupling reaches -10dB for most S_{12}, S_{13}, and S_{14} at the frequency band of interest. Reaching this reduction in the mutual coupling could be good, however, such distance adds a great impact on the antenna array size. Therefore, the authors conducted their study to the next section.

Next, the proposed antenna is arranged based on 2D configuration. The separation distances between the antenna elements are organized as presented in Fig. 1(c). The antenna array configuration is oriented sequentially, to reduce the effectively the mutual coupling between antenna elements. The proposed scenarios at different separation distance are included to realize the effects of that between the mutual coupling spectra only in terms of S_{12} in Fig. 4(a), S_{13} in Fig. 4(b), and S_{14} Fig. 4(c). Therefore, the separation distances (s) are changed from 10 to 30mm with a step 10mm. It is found after reaching 30mm distance, the mutual coupling reaches -10dB for most S_{12}, S_{13}, and S_{14} at the frequency band of interest. Reaching this reduction in the mutual coupling could be good, however, such distance adds a great impact on the antenna array size. Therefore, the authors conducted their study to the next section.

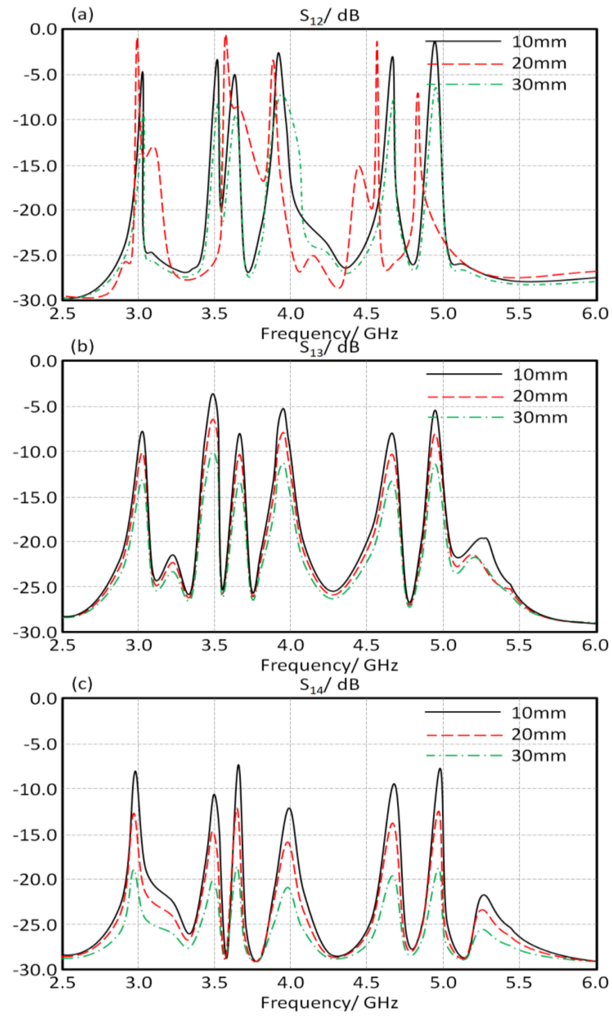

Fig. 4. Coupling effects of 2D configuration in terms of: (a) S_{12}, (b) S_{13}, and (c) S_{14} spectra.

Finally, the proposed antenna array is formed in shape of 3D configuration as shown in Fig. 1(d). Therefore, the proposed configuration with different separation distance (s) to monitor the mutual coupling between the antenna elements, S_{12}, S_{13}, S_{14}, as seen in Fig. 5(a)-5(c). The parameter (s) is changed from 1mm to 3mm with a step 1mm. It is recognized when s=2mm, the coupling in general is less than -15dB. However, when s=3mm, the coupling is reduced to less than -20dB. After reaching s=30mm, the mutual coupling becomes much less than -27dB for S_{12}, S_{13}, and S_{14} spectra at the frequency band of interest. Therefore, the authors considered s=3mm is enough for the design specification to provide mutual coupling of -20dB. Therefore, it is concluded according to the achieved results, the proposed antenna array based on 3D configuration shows excellent performances over other suggested configurations. This motivated us to move this configuration to the next step of the research.

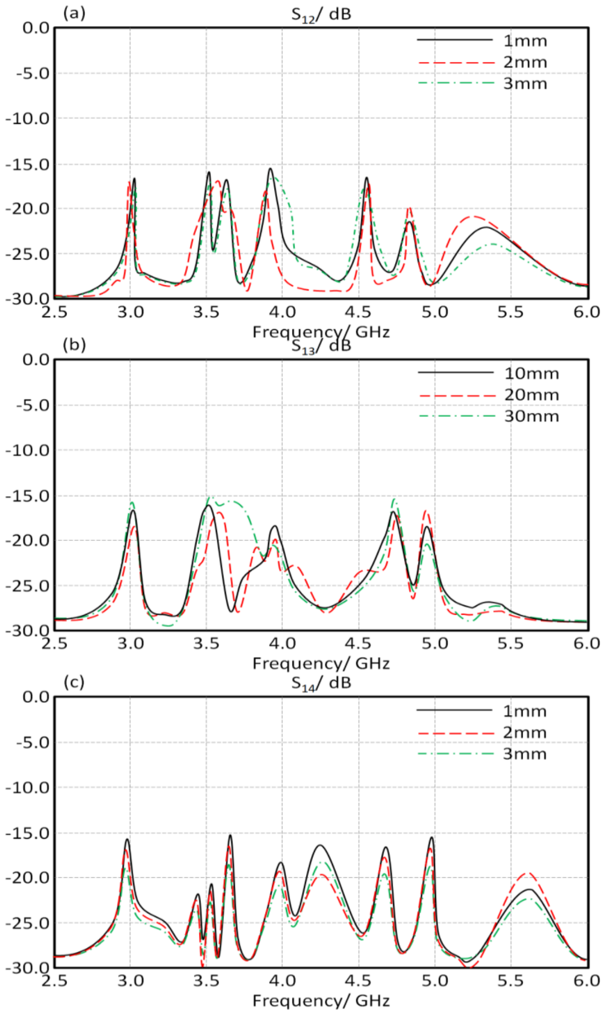

Fig. 5. Coupling effects of 2D configuration in terms of: (a) S_{12}, (b) S_{13}, and (c) S_{14} spectra.

IV. SOLAR CELL EFFECTS

In this section, the authors presented the effects of introducing the solar cell on the proposed antenna array performance in terms of S-parameters and gain spectra experimentally. The simulation study is not invoked in this work due to the knowledge limitations in the considered solar panel electromagnetic constitutive parameters. Thus, it is very important to point out that all previous simulations are attempted without considering the solar panel introduction. The proposed MIMO antenna system is introduced to the solar panel as shown in Fig. 1(f). It is found after applying the experimental study, the antenna performance is found to be insignificantly affected with the solar panel introduction. Indeed, the antenna gain is enhanced slightly at the desirable frequency bands. This is achieved by reducing the surface wave effects due to introducing the antenna array normally to the solar panel structure which realizes less surface wave effects [4].

Now, the solar panel effects on the proposed antenna array performance are described in term of S_{11} and gain spectra with and without the solar panel introduction. The antenna array position with respect to the solar panel is presented in Fig. 1(f). In Fig. 6(a), the obtained S_{11} from the proposed antenna array with and without solar panel is shown; it is found that matching bandwidth, $S_{11}\leq$-10dB, is insignificantly affected. The antenna gain spectra of the proposed antenna array are evaluated as seen in Fig. 6(b). It is found that the proposed antenna array gain is significantly not affected after the solar panel introduction in specific at 3.6GHz and 3.9GHz to realize a moderate gain that is suitable for 5G and other modern applications [13]. The effective correlation effects is not significantly increased after introducing the solar panel structure as shown in Fig. 6(c). The total affective reflection coefficient and total channel capacity losses are not changed at all as depicted in Figs. 6(d) and 6(e). The evaluated antenna diversity spectra are not increased after the solar panel introduction.

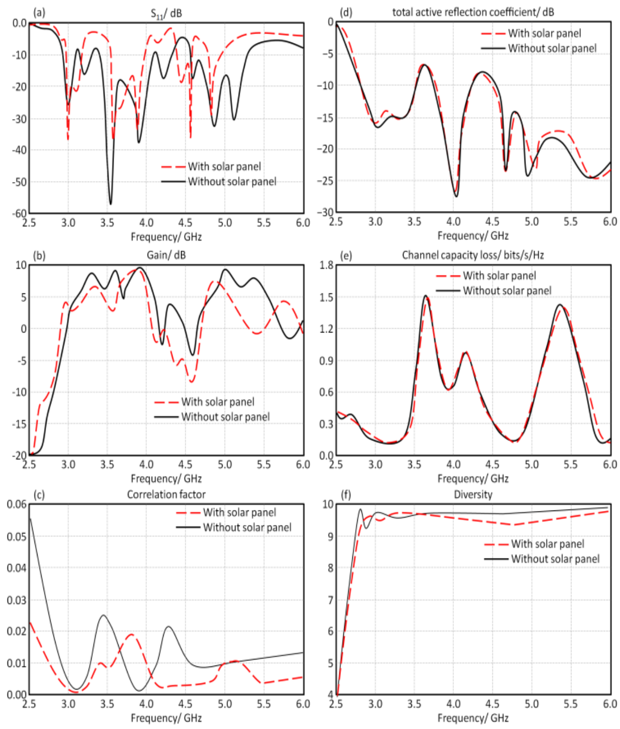

Fig. 6. Antenna array performance with and without solar panel introduction; (a) S_{11}, (b) gain, (c) correlation factor spectra, (d) total effective gain spectra, (e) Channel capacity losses, and (f) antenna diversity spectra.

V. Experimental Validation

In this section the proposed antenna array performance are measured using a vector network analyzer (37347A) and RF chamber. The proposed antenna array is fabricated, as seen in Fig. 1(f), and validated experimentally. The obtained results from the numerical analysis are compared to the experimental measurements. As seen in Figs. 7(a) and 7(b), the measured S_{11} and gain spectra are presented. It is found that the experimental results agree very well with those obtained from CST MWS. The other relative measurements of the S-parameters in terms of S_{12}, S_{13}, and S_{14} spectra as seen in Fig. 7(c)-7(e). It is validated that the maximum coupling is about -20dB after the solar panel introduction with excellent gain and bandwidth enhancements. The harvested solar energy of the proposed antenna with and without antenna introduction is presented in Fig. 7(f). The proposed MIMO antenna is put to the test in conjunction with a solar panel. As a result, before and after the solar panel integration, the measured I-V characteristics are given in Fig. 7(f). The I-V characteristics are not greatly impacted after and before the solar panel integration since the solar panel are placed properly to the antenna array. After the planned antenna is installed, the I-V characteristics of the solar panels are measured. This comparison is made to determine the impacts of the antenna on the solar panel in question. As a result, minimal effects on solar panel performance are discovered; see Fig. 7(f), after and before the antenna insertion. This is due to the antenna construction being located on the solar panel's rear panel. The solar energy is defined in the photo-current and photo-voltage curve.

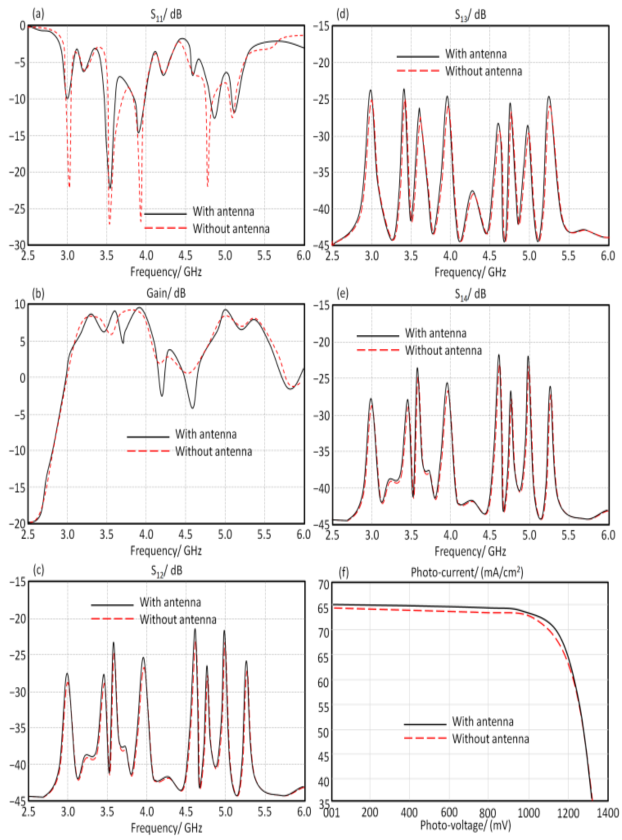

Fig. 7. Antenna performance with solar panel introduction; (a) S_{11}, (b) gain, (c) S_{12}, (d) S_{13}, (e) S_{14} spectra, and (f) I-V characteristics.

Based on the achieved results, the antenna performance is evaluated when introduced to real communication system based on QPSK modulation scheme. In this experiment, the total bit error rate (BER) and channel capacity are evaluated as shown in Fig. 8. The signal to nose ratio (SNR) are changed according to amount of the obtained power from the solar panel. According to our measurements, the total generated voltage was in the range of 0mV to 1000mV with constant current around 65mA as shown in Fig. 7(f). This gave us an indication of the total harvested energy from the considered solar panel. In such case, SNR is changed between 0dB to 60dB. It is found from the results in Fig. 8, a high SNR provide low BER, while, a low SNR would increase BER. In such case, this acquires an efficient solar panel for long use effectively. Nevertheless, the link budget effects could be significantly affected according to such knowledge. With the introduction of 5G the energy efficiency (Watt/Mbyte) of the 5G mobile radios many improvements were achieved. However, the total amount of the consumed energy is still increasing due to the sharply increasing data traffic that cause headache for the mobile network operators, since most of them operating not only 5G. It is obvious, frequency bands with higher gain are better than those with low gain to provide less chance of errors due to the noise effects.

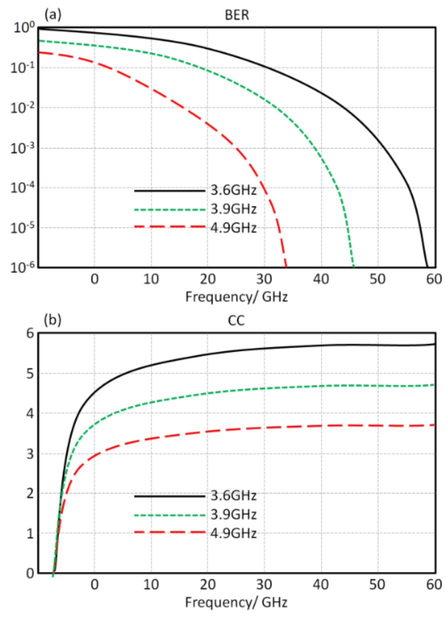

Fig. 8. Channel performance according to the solar panel I-V characteristics at different frequency bands. (a) BER and (b) CC calculations.

The proposed antenna radiation patterns are measured at 3.6GHz, 3.9GHz, and 4.9GHz as shown in Fig. 9. The measurements are given in both co- and cross-polarizations. It is concluded from the obtained results that the antenna is effectively very directive toward the broadside direction. Also, the introduction of the solar panel has no significant effects on the antenna directivity. It is compared in this section between the proposed antenna and other published results in Table I. It is found that the proposed antenna provides a highest miniaturized profile in comparison to other antenna designs based on 3D structures.

TABLE I
RESULTS COMPARISON WITH RESPECT OTHER PUBLISHED RESULTS.

Reference	Size/mm	Freq./GHz	Gain/dBi
23	70×30	3.78	-1.2
		8.24	0.56
24	100×100	2.45	3.45
25	130×130	5.6	5.8
26	60×70	2.45	3.4
27	90×90	5.8	6.7
28	60×40	2.45	2.3
29	90×90	2.45	1.2
30	22×30×72	2.45	2
32	40×50	2.45	2.1
33	20×30	3.5, 5	3, 3.5
This work	20×30	3.6	6.3
		3.9	7.9
		4.9	9

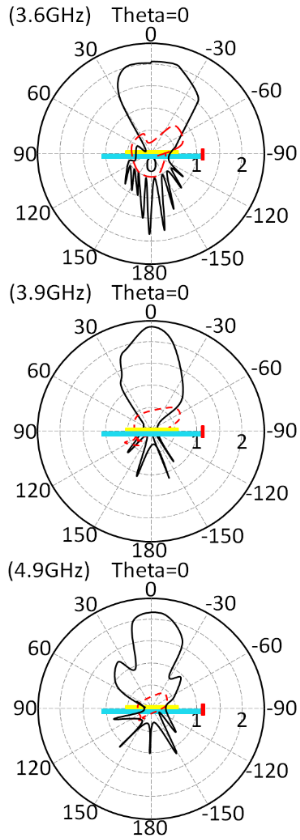

Fig. 9. Antenna radiation patterns measurements only after the solar panel introduction. Note: The discrete black line for co-polarization results and the red line for the cross-polarization results.

VI. CONCLUSION

In this work, a design of a 3D array antenna based solar panel integration for self-powered applications in modern wireless communication network. The proposed antenna array is structured as a cubical geometry with solar panel integration. Such integration is employed to achieve a self-powered node. The proposed antenna is designed to perform an excellent beam reconfiguration at sub-6GHz frequency bands. The proposed antenna is found to provide a moderate gain at 3.6GHz, 3.9GHz, and 4.9GHz. The proposed antenna array is found to provide coupling between the adjacent antenna elements bellow -20dB at the frequency bands of interest. The proposed antenna is fabricated and compared to the simulated results to achieve an excellent agreement between them. A solar panel is introduced to the proposed antenna array for self-powered applications. It is reviled that the proposed antenna system integration with solar panel shows no negative effects on the antenna performance. The antenna is introduced to a real wireless QPSK communication scheme. With such environments, we calculated the BER and CC with respect to the total obtained solar energy. This is done by introducing the amount of achieved power from the solar panel as SNR level to feed the QPSK scheme. We obtained within the limit of the harvested solar energy, acceptable BER and CC values. The antenna performance is validated theoretically and experimentally to arrive to an excellent agreement between the obtained results.

REFERENCES

[1] Abdulsattar, R. K.; Elwi, T. A.; Abdul Hassain, Z. A. A New Microwave Sensor Based on the Moore Fractal Structure to Detect Water Content in Crude Oil. *Sensors* 2021, 21, 7143. DOI: 10.3390/s21217143

[2] Alaukally M. N. N.; Elwi T. A.; Atilla D. C. Miniaturized flexible metamaterial antenna of circularly polarized high gain-bandwidth product for radio frequency energy harvesting. *Int J Commun Syst*. 2022; 35(3):e5024. DOI: 10.1002/dac.5024

[3] Yehia, S., Fatah, A.; Taher, F.; Elwi, T. A.; Fathy, M., Sree, A.; ... Limiti, E. (2023). Design of Compact Flexible UWB Antenna Using Different Substrate Materials for WBAN Applications. In *2023 Photonics and Electromagnetics Research Symposium (PIERS)*. Proceedings (373–378). DOI: 10.1109/PIERS59004.2023.10221357

[4] Ahmed Imad Imran, Taha Ahmed Elwi, and Ali J. Salim, "On the Distortionless of UWB Wearable Hilbert-Shaped Metamaterial Antenna for Low Energy Applications," *Progress In Electromagnetics Research M*, Vol. 101, pp. 219–239, 2021, DOI: 10.2528/PIERM20113008.

[5] S. M. Obaid, T. A. Elwi, and M. Ilyas, "Fractal Minkowski-Shaped Resonator for Noninvasive Biomedical Measurements Blood Glucose Test," *Progress in Electromagnetics Research C*, Volume 107, pp. 143–156, December 2020, http://dx.doi.org/10.2528/PIERC20072603.

[6] Elwi T. A., Al-Saegh A. M. Further realization of a flexible metamaterial-based antenna on indium nickel oxide polymerized palm fiber substrates for RF energy harvesting. *International Journal of Microwave and Wireless Technologies*. 2021;13(1):67–75. DOI: 10.1017/S1759078720000665

[7] Y. Alnaiemy, T. A. Elwi, L. Nagy, "An end fire printed monopole antenna based on electromagnetic band gap structure," *Automatika*, volume 61, issue 3, pp. 482–495, DOI: 10.1080/00051144.2020.1785783.

[8] T. A. Elwi, "Remotely Controlled Reconfigurable Antenna for Modern Applications", *Microwave and optical letters*, Volume 6, Issue 1, pp. 1–19, April 2020, DOI: 10.1002/mop.32505.

[9] A. Abdulmjeed, T. A. Elwi, and S. Kurnaz, "Metamaterial Vivaldi Printed Circuit Antenna Based Solar Panel for Self-Powered Wireless Systems," *Progress In Electromagnetics Research M*, Vol. 102, 181–192, 2021, http://dx.doi.org/10.2528/PIERM21032406

[10] M. A. Jawad, M. A. Elwi, E. Y. Salih, T. A. Elwi, and Zulkifly Abbas, "Monitoring the Dielectric Properties and Propagation Conditions of Mortar for Modern Wireless Mobile Networks," *Progress in Electromagnetic Research Letters*, Volume 89, pp. 91–97, January 2020, http://dx.doi.org/10.2528/PIERL19090912.

[11] P. Mishra and S. S. Pattnaik, "Metamaterial loaded fractal based interdigital capacitor antenna for communication systems," *Progress In Electromagnetics Research*, Vol. 70, pp. 127–134, 2018, http://dx.doi.org/10.2528/PIERM18032801.

[12] Y. Alnaiemy, T. A. Elwi, L. Nagy, "Mutual Coupling Reduction in Patch Antenna Array Based on EBG Structure for MIMO Applications", *Periodica Polytechnica Electrical Engineering and Computer Science*, Volume 1, number 4, pp. 1–11, September 2019, DOI: 10.3311/PPee.14379,

[13] T. A. Elwi, "Further Investigation on Solant-Rectenna based Flexible Hilbert-Shaped Metamaterials", *IET Nanodielectrics*, Volume 4, Issue 12, pp. 1–12, March 2020, DOI: 10.1049/iet-nde.2020.0013.

[14] H. M. Al-Sabbagh, T. A. Elwi, Y. Al-Naiemy, and H. M. Al-Rizzo, "A Compact Triple-Band Metamaterial-Inspired Antenna for Wearable Applications", *Microwave and Optical Technology Letters*, Volume 11, Number 2, October 2019, DOI: 10.1002/mop.32067.

[15] Z. A. Abdul Hassain, A. R. Azeez, M. M. Ali, and T. A. Elwi, “A Modified Compact Bi-Directional UWB Tapered Slot Antenna with Double Band-Notch Characteristics”, *Advanced Electromagnetics*, Volume 8, number 4, September 2019, http://dx.doi.org/10.7716/aem.v8i4.1130.

[16] T. A. Elwi, Z. A. AL-Hussain, O. Tawfeeq, “Hilbert Metamaterial Printed Antenna based on Organic Substrates for Energy Harvesting”, *IET Microwaves, Antennas & Propagation*, volume 12, number 4, pp. 1–8, June 2019, doi: 10.1049/iet-map.2018.5948.

[17] H. S. Ahmed and T. A. Elwi, “On the design of a reject band filter for antennas mutual coupling reduction”, *International Journal of RF and Microwave Computer-Aided Engineering*, volume 11, number 3, pp.1–11, April 2019, doi: 10.1002/mmce.21797.

[18] Y. Al Naiemy, T. A. Elwi, and L. Nagy, “An end fire printed monopole antenna based on electromagnetic band gap structure,” *Automatika*, vol. 61, no. 3, pp. 482–495, 2020, doi: 10.1080/00051144.2020.1785783.

[19] T. A. Elwi, D. A. Jassim, H. H. Mohammed, “Novel miniaturized folded UWB microstrip antenna-based metamaterial for RF energy harvesting,” *International Journal of Communication Systems*, Volume 1, Issue 2, January 2020, doi: 10.1002/dac.4305.

[20] R. R. K. Al-Taie et al., "On the Performance of a Composite Right Left Hand Electromagnetic Bandgap Structure," *2022 9th International Conference on Electrical Engineering, Computer Science and Informatics (EECSI)*, Jakarta, Indonesia, 2022, pp. 420–423, doi: 10.23919/EECSI56542.2022.9946487.

[21] Hussein, H.; Atasoy, F.; Elwi, T.A. Miniaturized Antenna Array-Based Novel Metamaterial Technology for Reconfigurable MIMO Systems. *Sensors* 2023, 23, 5871. doi: 10.3390/s23135871.

[22] Zainab S. Muqdad, Mohammad Alibakhshikenari, Taha A. Elwi, Zaid A. Abdul Hassain, Bal.S. Virdee, Richa Sharma, Salahuddin Khan, Nurhan Türker Tokan, Patrizia Livreri, Francisco Falcone, Ernesto Limiti, "Photonic controlled metasurface for intelligent antenna beam steering applications including 6G mobile communication systems", *AEU - International Journal of Electronics and Communications*, Vol. 166, 2023, 154652, ISSN 1434-8411, doi: 10.1016/j.aeue.2023.154652.

[23] M. R. I. Faruque, M. T. Islam, and N. Misran, “Design analysis of new metamaterial for EM absorption reduction,” *Progress In Electromagnetics Research*, vol. 124, pp. 119–135, 2012, http://dx.doi.org/10.2528/PIER11112301.

[24] H. Nakano, Low-profile Natural and Metamaterial Antennas: Analysis Methods and Applications. John Wiley & Sons, 2016.

[25] A. R. Al-tameemi et al., "A Novel Conformal MIMO Antenna Array based a Cylindrical Configuration for 5G Applications," *2022 9th International Conference on Electrical Engineering, Computer Science and Informatics (EECSI)*, Jakarta, Indonesia, 2022, pp. 446–451, doi: 10.23919/EECSI56542.2022.9946617.

[26] S. H. Ghadeer, T. A. Elwi and S. K. A. Rahim, "Compact MIMO Antenna Array for 5G Applications," *2022 9th International Conference on Electrical Engineering, Computer Science and Informatics (EECSI)*, Jakarta, Indonesia, 2022, pp. 399–402, doi: 10.23919/EECSI56542.2022.9946554.

[27] Ismail, M. M.; Elwi, T. A.; I Salim, A. J. (2022). A Miniaturized Printed Circuit CRLH Antenna-based Hilbert Metamaterial Array. *Journal of Communications Software and Systems*, 18 (3), 236–243, doi: 10.24138/jcomss-2022-0030.

[28] Y. Alnaiemy, T. A. Elwi and N. Lajos, "Enhancing the Microstrip Antenna Gain Using a Novel EBG Lens Based on a Single Layer," *2018 11th International Symposium on Communication Systems, Networks & Digital Signal Processing (CSNDSP)*, Budapest, Hungary, 2018, pp. 1–4, doi: 10.1109/CSNDSP.2018.8471786.

[29] Y. Alnaiemy, T. A. Elwi, L. Nagy, and T. Zwick, “A systematic analysis and design of a high gain microstrip antenna based on a single EBG layer,” *Infocommunications Journal*, vol. 10, no. 4, pp. 22–30, 2018, http://dx.doi.org/10.36244/ICJ.2018.4.4.

[30] Z. Al-Dulaimi, T. A. Elwi, and D. C. Atilla, “Design of a meander line monopole antenna array based hilbert-shaped reject band structure for MIMO applications,” *IETE Journal of Research*, pp. 1–10, 2020, doi: 10.1080/03772063.2020.1743207.

[31] Jwair, Marwah Haleem and Elwi, Taha A. (2023) Metasurface Antenna Circuitry for 5G Communication Networks. *Infocommunications Journal: A Publication of the Scientific Association for Infocommunications (HTE)*, 15 (2). pp. 2–7. ISSN 2061-2079, doi: 10.36244/ICJ.2023.2.1.

[32] H. Almizan, Z. A. A. Hassain, T. A. Elwi and S. M. Al-Sabti, "Controlling Gain Enhancement Using a Reconfigurable Metasurface Layer," *2021 12th International Symposium on Advanced Topics in Electrical Engineering (ATEE)*, Bucharest, Romania, 2021, pp. 1–6, doi: 10.1109/ATEE52255.2021.9425037.

[33] H. Almizan, Marwah Haleem Jwair, Yahiea Al Naiemy, Zaid A. Abdul Hassain, Lajos Nagy and Taha A. Elwi, "Novel Metasurface based Microstrip Antenna Design for Gain Enhancement RF Harvesting", *Infocommunications Journal*, Vol. XV, No 1, March 2023, pp. 2–8., doi: 10.36244/ICJ.2023.1.1.

[35] Y. A. Jassim, M. Çevik and T. A. Elwi, "10GHz Printed Circuit Antenna for Wireless Power Transfer Applications," *2023 5th International Congress on Human-Computer Interaction, Optimization and Robotic Applications (HORA)*, Istanbul, Turkiye, 2023, pp. 1–4, doi: 10.1109/HORA58378.2023.10156795.

[36] Ali, L., Ilyas, M., & Elwi, T. A. (2023). A metamaterial-based compact MIMO antenna array incorporating hilbert fractal design for enhanced 5G wireless communication networks. *Mathematical Modelling of Engineering Problems*, 10(3), 930–936, https://hdl.handle.net/20.500.12939/3672.

[37] M. H. Jwair et al., "Intelligent Metasurface Layer for Direct Antenna Amplitude Modulation Scheme," in *IEEE Access*, vol. 11, pp. 77 506–77 517, 2023, doi: 10.1109/ACCESS.2023.3297264.

Ammar Al-Adhami was born in Baghdad, Iraq, in 1993. He received the B.Sc. degree in Electrical Engineering from Al-Ma'amon University, Iraq in 2015, He received M.Sc degree from Gaziantep University, Turkey 2017. He received PhD degree from Gaziantep University, Turkey 2022. His research interests include wireless communication systems, microwave circuits design, wearable antennas, and antenna design.

Yasir Al-Adhami was born in Baghdad, Iraq, in 1990. He received the B.Sc. degree in Computer communication Engineering from Al-Mansour University, Iraq in 2012, He received M.Sc degree from Çankaya University, Turkey 2014. He received PhD degree from Gaziantep University, Turkey 2018. He is currently Lecturer in Electrical and Electronics Engineering Department of Gaziantep University. His research interests include Harvest Solar Energy and RF Energy for wireless applications, wireless communication systems, microwave circuits design, and antenna design.

Taha A. Elwi received his B.Sc. in Electrical Engineering Department (2003) (Highest Graduation Award), and Postgraduate M.Sc. in Laser and Optoelectronics Engineering Department (2005) (Highest Graduation Award) from Al-Nahrain University Baghdad, Iraq. From April 2005 to August 2007, he worked with Huawei Technologies Company, in Baghdad, Iraq. On January 2008, he joined the University of Arkansas at Little Rock and he obtained his Ph.D. in December 2011 in system engineering and Science. He is considered of Stanford University's top 2% scientists in 2022. His research areas include wearable and implantable antennas for biomedical wireless systems, smart antennas, WiFi deployment, electromagnetic wave scattering by complex objects, design, modeling, and testing of metamaterial structures for microwave applications, design and analysis of microstrip antennas for mobile radio systems, precipitation effects on terrestrial and satellite frequency re-use communication systems, effects of the complex media on electromagnetic propagation and GPS. His research is conducted to consider wireless sensor networks based on microwave terminals and laser optoelectronic devices. The nano-scale structures in the entire electromagnetic spectrum are a part of his research interest. Also, his work is extended to realize advancements in reconfigurable intelligent surfaces and control the channel performance. Nevertheless, the evaluation of modern physics phenomena in wireless communication networks including cognitive radio networks and squint effects is currently part of his research. His research interests include pattern recognition, signal and image processing, machine learning, deep learning, game theory, and medical image analysis-based artificial intelligence algorithms and classifications. He serves as an editor in many international journals and publishers like, MDPI, IEEE, Springer, and Elsevier. He is currently the head of the International Applied and Theoretical Research Center (IATRC), Baghdad Quarter, Iraq. Also, he has been a member of the Iraqi scientific research consultant since 2016. He is leading three collaborations around the world regarding biomedical applications using microwave technology. He is the supervisor of many funded projects and Ph.D. theses with corresponding of more than 150 published papers and holding 10 patents. He can be contacted at email: taelwi82@mail.com.